Suzanne D. Smith
Armstrong Laboratory
Wright-Patterson Air Force Base,
OH 45433-7901

Nonlinear Resonance Behavior in the Human Exposed to Whole-Body Vibration

The driving-point impedance technique was applied to identify nonlinear resonance behavior in the human exposed to sinusoidal vibration between 3 and 20 Hz at three acceleration levels. Up to four regions of resonance were observed. A significant decline in the first and fourth resonance frequency and the disappearance of the second resonance peak occurred with a fivefold increase in the acceleration level. A proposed, base-excited five degree-of-freedom model, representing major dynamic structures in the human, proved highly successful in simulating the typical impedance responses. The model was used to quantify the variations in the mass, stiffness, and damping characteristics associated with changes in the acceleration level. © *1994 John Wiley & Sons, Inc.*

INTRODUCTION

Studies have been conducted to evaluate the effects of whole-body vibration on human performance, tolerance, and health. These effects are of particular interest to the military because the wide variety of environments and tasks encountered by operations personnel include exposures to relatively long periods of vibration. The International Standards Organization (ISO) has formulated a guideline that provides numerical limits on acceleration levels and exposure duration at different frequencies for preserving comfort, working efficiency, and health (ISO 2631, 1985). The ISO Standard 2631 (1985) is widely used to assess a variety of vibration environments. The Military Standard 1472C (U.S. Dept. of Defense, 1981) references the ISO 2631 for designing military vehicles that are safe to operate. These exposures limits are primarily based on human tolerance data and field experience. The ISO has also published two standards that present available information on the application of the driving-point impedance (ISO 5982, 1981) and transmissibility (ISO 7962, 1987) techniques for evaluating human dynamic response. These two techniques can be used to collect information for developing analytical models of the human as a mechanical structure, and to design isolation systems including vehicle suspensions and seats. While indicating that the human body vibrated in the z axis does exhibit nonlinear characteristics, these two standards assume that under normal gravity and acceleration amplitudes the human behaves as a linear system. In general, the impedance technique and a related quantity, the apparent or effective mass (ratio of transmitted force to input acceleration), assume that the respective vibrating structure exhibits linear dynamic response behavior under steady-state

Received August 23, 1993; Accepted March 18, 1994.
Shock and Vibration, Vol. 1, No. 5, pp. 439–450 (1994)

CCC 1070-9622/94/050439-12

loading conditions. However, a limited number of studies have used these two ratios to describe changes in the frequency response characteristics relative to the loading magnitude. Two recent studies applied the apparent or effective mass technique to evaluate the effects of the acceleration level on human whole-body response. Hinz and Seidel (1987) exposed male subjects to sinusoidal frequencies between 2 and 12 Hz and found that the location of the primary resonance frequency shifted from 4.5 to 4.0 Hz with increases in the acceleration level from 1.5 to 3.0 ms^{-2} rms. Using quasirandom vibration with frequency components ranging from 0.25 to 25 Hz, Fairley and Griffin (1989) observed a decrease in the mean resonance frequency from 6 to 4 Hz with increases in acceleration from 0.25 to 2.0 ms^{-2} rms. The subject pool included both males and females. The investigators concluded that the decrease in resonance frequency at higher acceleration levels is due to reduced stiffness resulting from greater movement in the musculoskeletal system. Studies have been conducted at the Armstrong Laboratory to investigate the effects of acceleration magnitude on the response of the small male primate Rhesus monkey. Although Slonim (1981) did not report any significant effect due to variations in the acceleration magnitude, Smith and Kazarian (1994) identified a significant decline in the primary resonance frequency from a mean of 16.8 to 12.2 Hz with acceleration increases from 0.694 to 3.47 ms^{-2} rms (0.1–0.5 *g* peak). They also observed a second resonance peak at about 5 Hz that had not been previously reported. Using a three-mass, two degree-of-freedom (2DOF) model, the investigators associated the decrease in the resonance frequency at the higher acceleration level with a decrease in the stiffness of the upper torso.

Previous studies have been conducted under a variety of test conditions and assumptions. In particular, emphasis has been placed on studying the nonlinear behavior associated with the primary resonance peak and not necessarily in identifying and modeling the behavior of any additional resonances that may or may not be affected by the acceleration magnitude. This article describes the application of the driving-point impedance technique to identify regions of resonance and their variations as a function of acceleration level in the human. A mathematical model is proposed for quantifying the dependence of the mass, stiffness, and damping characteristics on the acceleration level.

METHODS AND MATERIALS

Vibration Tests, Data Collection, and Reduction

An Unholtz–Dickie electrodynamic vertical motion simulator was used to produce the *z*-axis vibration. A specially designed human test seat was constructed that would respond as a pure mass over the frequency range of concern and included a horizontal seatpan, a seatback oriented at 90° from the seatpan, a lapbelt, and a double shoulder harness. Transmitted force was measured by three equally spaced load cells located between the seatpan and the vibrator platform. A piezoresistive accelerometer was attached beneath and in the center of the seatpan for measuring the input acceleration magnitude. A piezoelectric accelerometer, similarly attached to the seatpan, was used to measure the input acceleration phase. A computer software package was developed to provide the capability for the generation of sinusoidal frequencies at selected acceleration levels, the simultaneous collection of load cell and accelerometer data, and the calculation of magnitude and phase relations using a fast Fourier transform (FFT). The initial signal conditioning system provided amplification and filtering at 100 Hz of all transducer output. A second set of programmable modules was primarily used to sample and hold all analog data. The data was digitized at 1024 Hz. For each frequency, data were collected for 2 s. The seat input velocity was calculated from the seat input acceleration data. The driving-point impedance magnitude and phase at each load cell site and for each frequency was calculated as the ratio and phase between the transmitted force and input velocity, respectively. To obtain the subject's impedance, the complex impedance of the seat (measured previously) was subtracted from the complex impedance of the combined seat/subject at each site. The resultant impedances calculated at the three load cell sites were mathematically summed to obtain the total complex impedance of the subject. The subject impedance magnitude and phase were calculated as the absolute value of the complex ratio and the arc tangent between the imaginary and real components of the complex value, respectively.

Impedance frequency response profiles were collected by exposing four male subjects to discrete sinusoidal frequencies between 3 and 20 Hz (3–10 Hz in 1-Hz increments and at 12, 14, 15, 16, 18, and 20 Hz) at the selected acceleration

level. The subjects were tested four times each at 0.347, 0.694, and 1.734 ms^{-2} rms (0.05, 0.10, and 0.25*g*s peak) for a total of 16 frequency response profiles at each of the three acceleration levels.

During the vibration exposures, the subjects were loosely restrained by the lapbelt and shoulder harness primarily for safety considerations. The subjects were instructed on the importance of maintaining a consistent and erect posture during data collection. Consistency in posture was optimized with the use of the restraint system and the presence of the seatback. The subjects thighs rested on the seatpan in a comfortable and natural position with the hands placed in the subject's lap. The seat/restraint configuration did not include a footrest. Visual observations of the subjects were made during the vibration exposures. Any notable increases or decreases in the motions of specific anatomical regions, including the chest, head, neck, and legs, were documented. Subjects were also asked to comment on any pronounced localized sensation of vibration.

RESULTS

Impedance Response and Resonance Behavior

Figure 1 illustrates the impedance magnitude and phase response for one subject at the three acceleration levels. The figure shows up to four relatively distinct peaks in the magnitude profiles between 3 and 20 Hz with the most distinguishable peaks being observed for the lowest acceleration level (0.347 ms^{-2} rms). The peaks in the magnitude data and the associated frequencies were used to define the impedance resonances. Based on similar observations of these peaks in all 48 impedance magnitude profiles, four regions of resonance were defined as follows: region one ranged from 5 to 8 Hz; region two ranged from 7 to 9 Hz; region three ranged from 12 to 14 Hz; and region four ranged from 15 to 18 Hz. The phase profiles showed a rapid decline through the first region of resonance. Above about 7 Hz, the phase either leveled off or showed abrupt fluctuations between 0 and 30° which coincided with the occurrence of the remaining resonance peaks observed in the magnitude data. Except for one test at the lowest acceleration level, the phase did not cross 0 between 3 and 20 Hz. Figure 1 illustrates that, for the lowest acceleration level, the primary or highest resonance peak was not always identified as the first resonance peak associated with region one. For over 50% of the tests conducted at 0.347 ms^{-2} rms, the primary or highest resonance peak occurred in the second region of resonance between 7 and 9 Hz; the first peak was observed at a relatively lower magnitude between 5 and 7 Hz.

Figure 2 illustrates the mean and standard deviation (SD) for the resonance frequencies observed in each region at each of the three acceleration levels. The SDs for the second and third regions at 0.694 ms^{-2} rms and the SD for the third region at 1.734 ms^{-2} rms were 0 as depicted in the

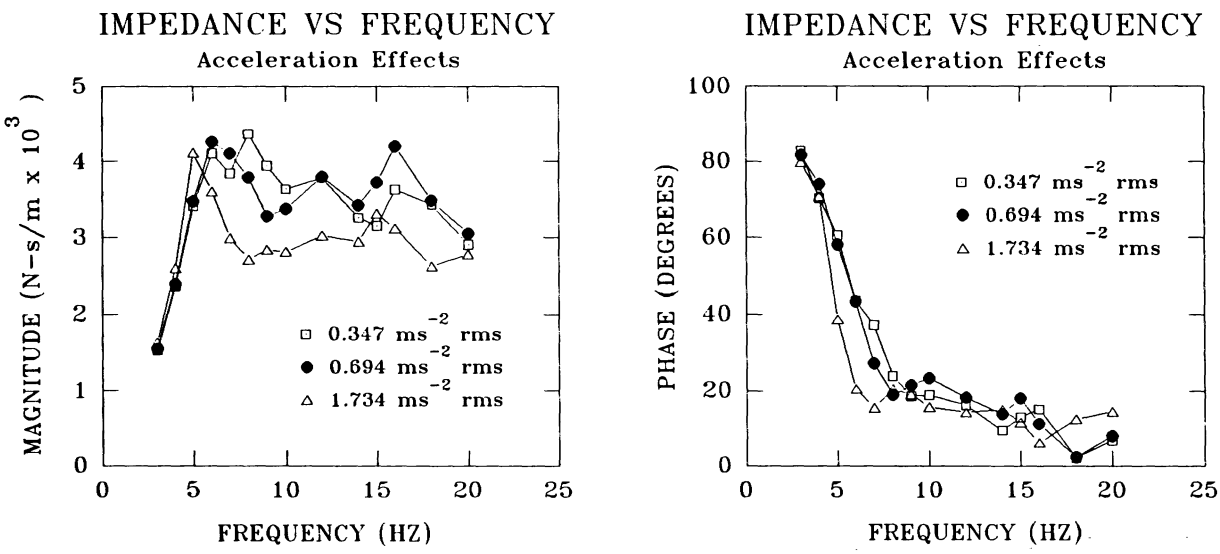

FIGURE 1 Typical impedance magnitude and phase responses at the three acceleration levels (one subject).

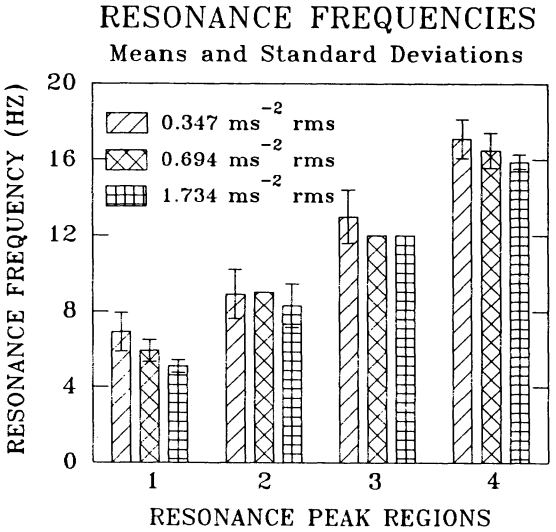

FIGURE 2 Mean resonance frequencies for the four peak regions.

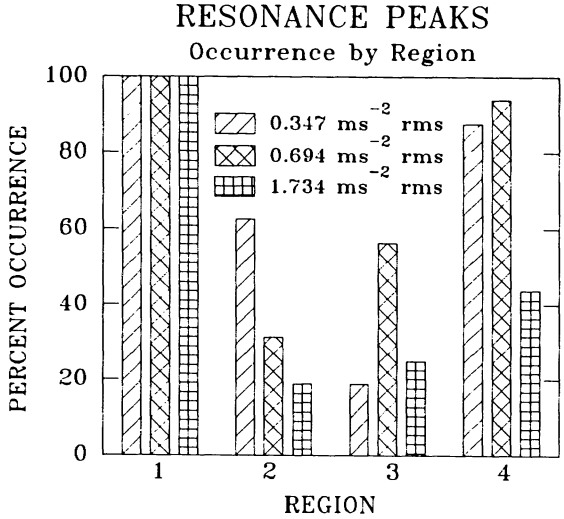

FIGURE 3 Occurrence of resonance peaks by region.

figure. The mean resonance frequency for the first resonance region shifted downward from 6.8 Hz at 0.347 ms^{-2} rms to 5.9 Hz at 0.694 ms^{-2} rms and to 5.2 Hz at 1.734 ms^{-2} rms. Figure 2 shows that all three mean resonance frequencies for the second resonance peak (region two) fell within ±1 SD showing no significant effect of acceleration level. A comparison between the lowest and highest acceleration levels (0.347 and 1.734 ms^{-2} rms) did show a significant decline in the resonance frequencies associated with the first and fourth regions of resonance with increasing acceleration. Analysis of variance corroborated these findings at the 5% confidence level. The mean value for the third resonance frequency also tended to be higher and more variable at the lowest acceleration level (0.347 ms^{-2} rms). In addition to these observations, the occurrence of the three resonance regions located beyond the first peak depended on the acceleration level. Figure 3 depicts the percentage occurrence of the four regions of resonance for each acceleration level. In summary, although the mean resonance frequency of the second peak (region two) did not appear to be affected by the acceleration level, the occurrence of this peak was greatly reduced at the higher acceleration levels. The lowest incidence of resonance behavior occurred in the impedance response profiles collected at the highest acceleration level (1.734 ms^{-2} rms). For the fourth resonance region, the occurrence of the peak was also greatly reduced at the highest acceleration level. The third resonance peak was most prevalent at 0.694 ms^{-2} rms.

Preliminary Modeling of Impedance Data

The observation of up to four regions of resonance in the human response data collected in this study required, at a minimum, a 4DOF model for simulating the response. Because the impedance calculations were associated with the response of a base-excited system, the model was defined as a base-excited 5DOF system for this study. Figure 4 illustrates the proposed model. The impedance measurements obtained in this study represent the combined effects of

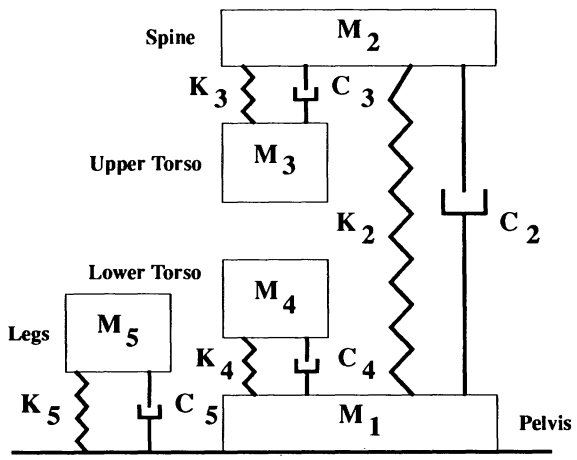

FIGURE 4 Base-excited 5DOF model.

the dynamic behavior of the body's major anatomical structures. The following presents the rationale for the particular formulation presented in Fig. 4 based on the available literature, the visual observations of body segment motions, the verbal responses of the subjects, and the specific characteristics of the resonance behavior observed in the impedance curves collected in this study. The impedance response results for the Rhesus monkey (Smith, 1992; Smith and Kazarian, 1994) indicated that modeling the pelvis as an inert mass component moving with the seat, as initially presented by Broderson and von Gierke (1971), results in relatively higher impedance magnitude values at higher frequencies and can prevent the impedance phase from crossing 0. Their approach assumed that any stiffness and damping contributions from the soft tissues located between the seat and the ischial tuberosities were insignificant relative to the measurement of driving-point impedance and the reactive response of other body structures for the tested frequency range and acceleration levels. Based on the results for the human, the same assumptions were made in this study. Referring to the lumped-parameter model in Fig. 4, the rigid musculoskeletal components of the pelvis moving with the set are represented by element M_1 (subsystem one).

Peak transmissibility to the head has been observed by many investigators to occur between 4 and 8 Hz (Coermann, 1961; Mertens, 1978; Wilder et al., 1982; Hagena et al., 1986; ISO 7962, 1987). A few researchers, however, have reported that the actual resonance of the head relative to the trunk occurs between 17 and 25 Hz (Guignard, 1972; Hagena et al., 1986), although the transmissibility amplitude was quite low and usually measured as unity or less. At the higher frequencies beyond 12 Hz the subjects in this study indicated that there was a very strong sensation of vibration in the face. This was also quite evident from visual observation. Several subjects also reported that they were having difficulty focusing. The head constitutes a relatively small mass as compared to other dynamic structures in the body and is located some distance from the point of load application and the collection of impedance data. For this study, it was assumed that any resonance behavior of the head would not significantly contribute to the measured response at the seat. Depending on the acceleration level, the majority of data collected in this study did show a distinct peak between 15 and 18 Hz. Hagena et al. (1986) observed the highest transmissibility between the os sacrum and the sixth thoracic vertebra as well as the seventh cervical vertebra around 18 Hz. These results strongly suggested that the spinal column, particularly the thoracic spine, may have been the primary contributor to the impedance peak observed in the fourth region. For the preliminary modeling of the impedance response, the musculoskeletal components associated with the spinal column were modeled as a single lumped subsystem (subsystem two) represented by elements M_2, K_2, and C_2 and identified as the spine in Fig. 4.

Guignard and Irving (1960), using transmissibility measurements and high-speed cinematography, concluded that the response around 5 Hz was primarily due to resonance of the upper torso and shoulder girdle. In this study, visual observations and verbal communications with the subjects further confirmed the occurrence of relatively higher motions in the chest and shoulders in the frequency range of the first region of resonance (5–7 Hz). Previous investigators have assumed that the thoracic and abdominal viscera represent a coupled system based on data collected in the supine position (Coermann et al., 1960). It is not clear to what extent the motions of the soft tissues and organs of the abdomen may be coupled with the response of the thoracic viscera in the seated upright posture during vertical vibration. Subsystem three, represented by elements M_3, K_3, and C_3, was coupled to the spinal subsystem and represents the combined response characteristics of the organs and soft tissues contained within the rib cage and the shoulders. Based on the available data and on anatomical considerations, the visceral components include the thoracic viscera as well as those abdominal organs and tissues that lie in close proximity or are attached to the diaphragm, including the liver and stomach, and which are contained within the lower boundaries of the rib cage. Subsystem three is identified as the upper torso in Fig. 4.

Associating anatomical structures with the resonance behavior observed in regions two and three was more difficult and, as a first approximation, primarily based on visual observations, the verbal comments of the subjects, and the particular characteristics of the resonance peaks. Depending on the acceleration level, both peaks were relatively distinct in appearance indicating that the reactive forces associated with the mo-

tions of the respective anatomical structure(s) were being transmitted back to the seat and not dampened out or masked by the reactions of the upper torso/spine system (subsystems two and three). In order to simulate the observed resonance behavior, both subsystems were represented as anatomical structures or regions whose motions were uncoupled from the motions of the upper torso/spine. In this study, it was observed that the largest relative motions of anatomical structures or regions shifted from the upper torso to the lower torso below the waist at higher frequencies beyond the first resonance peak. Subjects also noted a strong sensation of the vibration in the lower torso in the frequency range associated with the third resonance peak. The soft tissues and muscles located in the pelvic area, including those of the hips, buttocks, and upper thighs, as well as the pelvic viscera, could comprise a significant reactive mass located at the seat or point of load application. Coermann (1961) observed a small peak at about 10 Hz in his impedance measurements using eight subjects. The results of his study suggested that this peak may be associated with motions in the pelvis. Again, the distinct peak observed in region three in many of the profiles strongly supports, as a first approximation, the addition of a second uncoupled subsystem. Subsystem four (M_4, K_4, and C_4) represents the lower torso in Fig. 4 and includes the viscera, soft tissues, and muscles located in the pelvic area, and the lower abdominal viscera, including the intestines. The subsystem was attached to the rigid components of the pelvis (M_1) with the motion of the subsystem being solely dependent on the motion of the seat and uncoupled from the motions of the upper torso and spine. This assumed, as a first approximation, that any stiffness and damping behavior occurring between the upper torso/spine and lower torso had a negligible effect on the motions of the two anatomical regions. Until further data is collected, associating any specific anatomical structures with the response observed in region four is speculative.

The legs comprise another major anatomical structure located at the seat and capable of dynamic motion during seated whole-body vibration. Because the entire weight of the thighs rested directly on the seatpan with the lower legs hanging freely, it was speculated that their contribution to the impedance measurement could be significant. Fairley and Griffin (1989), who evaluated the use of a footrest, did not observe any resonance peaks in the apparent mass between 7 and 9 Hz without the footrest at 1.0 ms^{-2} rms, which is consistent with the results of this study at a comparable acceleration level. However, they did observe that the primary or first resonance peak was higher in magnitude for the unsupported feet and that there was a slight increase in the apparent mass at frequencies above 10 Hz with increased thigh/seat contact (i.e., lowering of the footrest). Mertens (1978), although not specifically addressing the effects of the legs on the impedance response, also modeled the thighs as a reactive mass subsystem located at the seat and uncoupled from the motions of the other anatomical structures. Using the model parameters presented by Mertens (1978), the undamped natural frequency was calculated to be 9 Hz at 3.924 ms^{-2} rms. Motions in the legs were observed to be quite pronounced below 10 Hz, providing some physical evidence for their influence in the generation of the second peak between 7 and 9 Hz. In the proposed model, the legs were modeled as subsystem five in Fig. 4 and represented by elements M_5, K_5, and C_5. Their motion was assumed to be independent of the motions of the other subsystems represented in Fig. 4 for the acceleration levels and frequencies used in this study.

The general approach for deriving the complex impedance equation is outlined in Neubert (1987). For the model, the differential equations of motion are:

$$M_1\ddot{x}_1 + K_2(x_1 - x_2) + C_2(\dot{x}_1 - \dot{x}_2) + K_4(x_1 - x_4) + C_4(\dot{x}_1 - \dot{x}_4) + K_5(x_1 - x_5) + C_5(\dot{x}_1 - \dot{x}_5) = F_T \quad (1)$$

$$M_2\ddot{x}_2 + K_2(x_2 - x_1) + C_2(\dot{x}_2 - \dot{x}_1) + K_3(x_2 - x_3) + C_3(\dot{x}_2 - \dot{x}_3) = 0 \quad (2)$$

$$M_3\ddot{x}_3 + K_3(x_3 - x_2) + C_3(\dot{x}_3 - \dot{x}_2) = 0 \quad (3)$$

$$M_4\ddot{x}_4 + K_4(x_4 - x_1) + C_4(\dot{x}_4 - \dot{x}_1) = 0 \quad (4)$$

$$M_5\ddot{x}_5 + K_5(x_5 - x_1) + C_5(\dot{x}_5 - \dot{x}_1) = 0. \quad (5)$$

By defining

$$F_T(t) = F_T e^{i\omega t} \quad (6)$$

$$x_j = \frac{V_j e^{i\omega t}}{i\omega} \quad (7)$$

$$\dot{x}_j = V_j e^{i\omega t} \quad (8)$$

$$\ddot{x}_j = i\omega V_j e^{i\omega t}, \quad (9)$$

where $F_T e^{i\omega t}$ is the transmitted force at the platform and $V_j e^{i\omega t}$ is the velocity of mass M_j, and substituting Eqs. (6), (7), (8), and (9) into Eqs. (1)–(5), the complex driving-point impedance can be expressed by solving for $Z_T = F_T/V_1$:

$$Z_T = \left[i\omega M_1 + \frac{K_2}{i\omega} + C_2 + \frac{K_4}{i\omega} + C_4 + \frac{K_5}{i\omega} + C_5\right] - \frac{\left[\frac{K_2}{i\omega} + C_2\right]^2}{\left(i\omega M_2 + \frac{K_2}{i\omega} + C_2 + \frac{K_3}{i\omega} + C_3\right) - \frac{\left(\frac{K_3}{i\omega} + C_3\right)^2}{\left(i\omega M_3 + \frac{K_3}{i\omega} + C_3\right)}} - \frac{\left[\frac{K_4}{i\omega} + C_4\right]^2}{\left[i\omega M_4 + \frac{K_4}{i\omega} + C_4\right]} - \frac{\left[\frac{K_5}{i\omega} + C_5\right]^2}{\left[i\omega M_5 + \frac{K_5}{i\omega} + C_5\right]}. \tag{10}$$

The impedance magnitude is the absolute value of Eq. (10) and the phase angle between F_T and V_1 is given by the arc tangent of the ratio of imaginary to real components in Eq. (10).

The undamped natural frequencies can be calculated for the fixed-base five-mass, 4DOF system. From Eqs. (4) and (5), the undamped natural frequencies for subsystems four (lower torso) and five (legs), f_{04} and f_{05}, are easily calculated as

$$f_{04} = \sqrt{\frac{K_4}{M_4}} \tag{11}$$

$$f_{05} = \sqrt{\frac{K_5}{M_5}}. \tag{12}$$

For the coupled subsystems representing the upper torso and spine, the undamped natural frequencies can be calculated from Eqs. (2) and (3) and are given by

$$f_{02}^2 = \frac{\left[\frac{K_2}{M_2} + \frac{K_3}{M_3} + \frac{K_3}{M_2}\right] + \sqrt{\left[\frac{K_2}{M_2} + \frac{K_3}{M_3} + \frac{K_3}{M_2}\right]^2 - \frac{4K_2K_3}{M_2M_3}}}{8\pi^2} \tag{13}$$

$$f_{03}^2 = \frac{\left[\frac{K_2}{M_2} + \frac{K_3}{M_3} + \frac{K_3}{M_2}\right] - \sqrt{\left[\frac{K_2}{M_2} + \frac{K_3}{M_3} + \frac{K_3}{M_2}\right]^2 - \frac{4K_2K_3}{M_2M_3}}}{8\pi^2}, \tag{14}$$

where f_{02} represents the undamped natural frequency of the spinal column subsystem (spine) and f_{03} represents the undamped natural frequency of the chest/shoulders subsystem (upper torso).

The preliminary approach used to determine the effectiveness of this model in simulating both the magnitude and phase data included making an initial estimate of the masses for the anatomical structures represented in the model. In addition, initial values for the stiffness coefficients were determined based, in part, on estimating the undamped natural frequency of those subsystems whose motions were independent of the motions of other represented structures (subsystems four and five in Fig. 4). It was assumed that the undamped natural frequencies of the subsystems would approximate the resonance frequencies. The damping coefficients were adjusted to best approximate the magnitude of the resonance peaks. This procedure was applied to the results illustrated in Fig. 2 for all three acceleration levels. These results were considered as representative of the variability in the impedance data and

could demonstrate the capability of the model for simulating the response behaviors observed in this study.

Preliminary Modeling Results

Figure 5 shows the modeling results for the three acceleration levels. The base-excited 5DOF model proved highly effective in simulating the impedance magnitude and phase at all three acceleration levels. Although some discrepancy was observed between the actual and simulated phase between 10 and 15 Hz, the shapes of the curves were quite similar. Figure 6 identifies the model parameters associated with each acceleration level. Except for the legs (subsystem five),

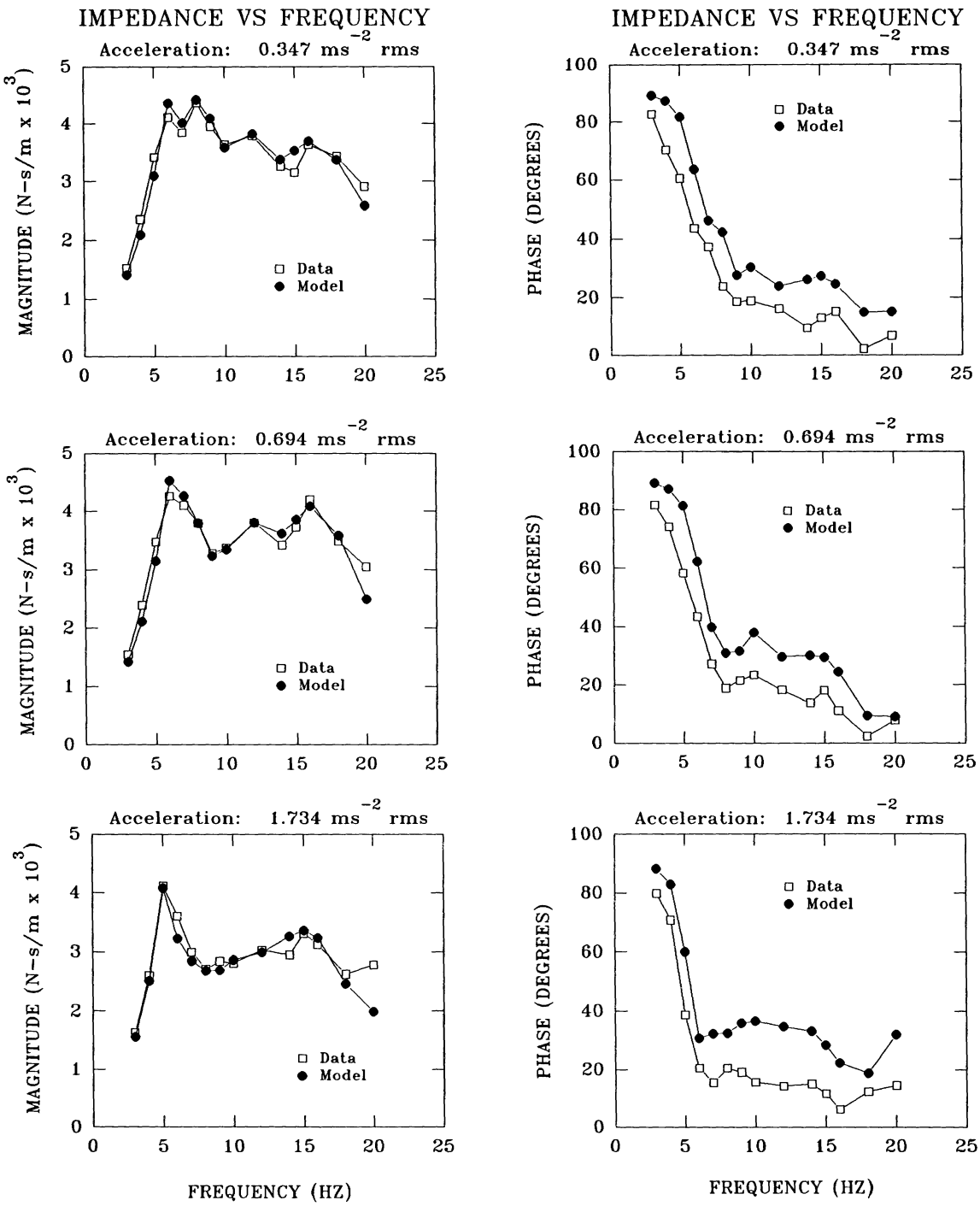

FIGURE 5 Modeling results for the three acceleration levels.

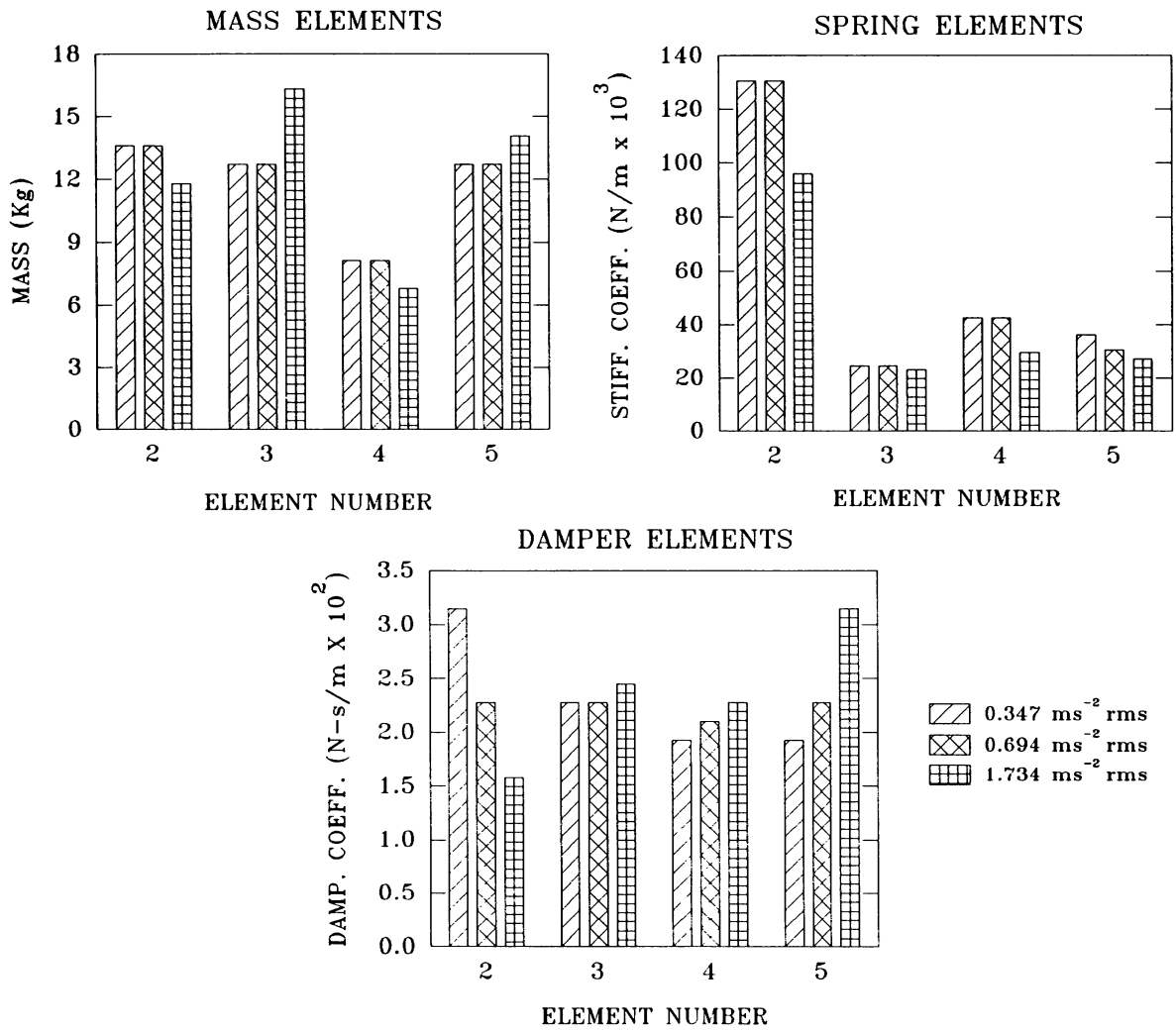

FIGURE 6 Parameter values from the base-excited 5DOF model.

the difference between the responses at 0.347 and 0.694 ms^{-2} rms was the result of changes in the damping characteristics associated with the respective anatomical structure. For the coupled upper torso and spine, the dynamic properties of the chest and shoulder region did not change, and damping in the spinal column was decreased, the effect being to increase the magnitude of the fourth peak at 0.694 ms^{-2} rms. The figure also shows that the elimination of the second resonance peak at the higher acceleration levels (0.694 and 1.734 ms^{-2} rms) coincided with an increase in the damping behavior of the legs (subsystem five). The significant decline in the location of the first and fourth resonance peaks at the highest acceleration level (1.734 ms^{-2} rms) was primarily influenced by an increase in the mass associated with the chest structures (subsystem three) and a substantial decline in the stiffness and damping properties of the lumped spinal components (subsystem two). In summary, the results of modeling showed that the reduced magnitude and lack of observable resonance behavior in the second and third frequency regions at the highest acceleration level (1.734 ms^{-2} rms) were primarily produced by a combination of decreased stiffness and increased damping in the associated anatomical structures.

Undamped Natural Frequencies and Resonance Behavior

The resonance frequency is defined as the frequency at which the response of a system is maximum for forced vibration. The undamped natural frequency is the frequency of free vibration resulting from the elastic and inertial forces of a system. The differences between these frequen-

cies are dependent on the coupling and damping in the system. Table 1 lists the undamped natural frequencies calculated for the fixed-based system using Eqs. (11)–(14) and the model parameters depicted in Fig. 6. The location of the resonance peaks associated with all subsystems (upper torso/spine) coincided closely with the undamped natural frequencies. For the first and fourth resonance region associated with the coupled subsystems (upper torso/spine), the undamped natural frequency showed a 1-Hz decrease at the highest acceleration level, similar to the decrease observed in Fig. 1 for the location of the resonance peaks. The figure also shows that the undamped natural frequency, calculated from the model parameters associated with the legs subsystem, decreased with increasing acceleration level and appeared to be primarily due to a decrease in the stiffness of the legs. Although the increase in damping may have influenced the magnitude of the leg response, the lowering of the undamped natural frequency suggests that any resonance behavior associated with the legs occurred as part of the response observed in region one between 5 and 7 Hz.

DISCUSSION

The results of this study agree with the results of Hinz and Seidel (1987) and Fairley and Griffin (1989) for the human, and Smith and Kazarian (1994) for the Rhesus monkey, in which the primary or first resonance frequency declined with increasing acceleration level. In addition, resonance behavior was also observed in up to three other frequency regions and clearly appeared to be dependent on the acceleration level. Although other investigators have observed resonance behavior in the frequency regions beyond the first resonance peak (5–7 Hz) (Coermann, 1961; ISO 5982, 1981; Wilder et al., 1982; Hagena et al., 1986; Fairley and Griffin, 1989), their observations have not been as consistent or as pronounced as the results of this study. Fairley and Griffin (1989) observed a peak in the apparent mass response in the vicinity of 10 Hz in most of their subjects but the behavior was not distinct. The frequency associated with this magnitude peak, when observed, decreased with increasing acceleration level. Coermann (1961) observed small impedance peaks at about 10 and 15 Hz in one subject seated erect but the mean impedance calculated for eight subjects only showed the small peak at about 10–11 Hz. Again, these peaks were relatively small compared to the behavior observed in this study. The clear observation of a peak between 7 and 9 Hz at 0.347 ms^{-2} rms in this study has not been reported elsewhere for the human although others have considered the legs as having an influence on the dynamic response characteristics (Mertens, 1978; Fairley and Griffin, 1989). It appeared that Coermann (1961) and Wilder et al. (1982) also allowed the legs to hang freely in their studies; however, the acceleration levels used were not clearly defined. It is assumed that the levels were greater than 0.347 ms^{-2} rms because the characteristic peak observed in region two of this study was not observed in their results. In this study it was speculated that the inclusion of a footrest would have reduced the dynamic loading of the legs against the seatpan and eliminated the second resonance peak at 0.347 ms^{-2} rms.

The base-excited 5DOF model proposed in this study was highly effective in simulating the representative impedance responses at three acceleration levels with some discrepancies observed for the phase. However, even though the parameter selections were primarily based on the characteristics of the magnitude response (i.e., resonance peaks), the phase results were quite reasonable. The model was used to quantify changes in the mass, stiffness, and damping characteristics of the lumped anatomical structures as a function of the input acceleration level. The mass and stiffness parameters generated by the model were used to calculate the four undamped natural frequencies associated with the lumped anatomical structures represented by the reactive subsystems illustrated in Fig. 4. The results showed that there was at least a 1-Hz decrease in all of the undamped natural frequencies with a fivefold increase in the acceleration level that coincided with the observed reductions in the resonance frequencies associated with the upper torso/spine (subsystems two and three). In the

Table 1. Undamped Natural Frequencies Calculated from Modeling Parameters

	Acceleration Level (ms^{-2} rms)		
Subsystem	0.347	0.694	1.734
2 (spine)	17.3 Hz	17.3 Hz	16.2 Hz
3 (upper torso)	6.3 Hz	6.3 Hz	5.3 Hz
4 (lower torso)	11.5 Hz	11.5 Hz	10.5 Hz
5 (legs)	8.5 Hz	7.8 Hz	7.0 Hz

model, the motions of the coupled subsystems were dependent on each other as well as on the motion of the seat. For the coupled subsystems it was found that changes in the mechanical parameters of one subsystem could dramatically affect the resonance behavior associated with the other coupled subsystem. Approximately 44% of the profiles at the highest acceleration level did exhibit resonance behavior in the fourth region and a reduction in the first and fourth resonance frequency. In order to lower the first resonance frequency at the higher acceleration level, the initial and most obvious approach was to lower the stiffness of the chest subsystem, however, reductions in the chest stiffness to the extent of lowering the resonance frequency to 5 Hz produced a higher magnitude for the fourth peak that did not necessarily occur at 15 Hz. Attempts to change the stiffness and damping characteristics of the spine resulted in the elimination of the fourth peak. By increasing the relative mass contribution of the chest structures at the higher acceleration level (i.e., changing the mass ratio between the coupled subsystems), the first resonance frequency was easily reduced without eliminating the fourth peak. Subsequently, the stiffness associated with the spinal column structure was reduced, further supporting the conclusions of Fairley and Griffin (1989) that "the greater movement that occurs with high magnitudes of vibration reduces the stiffness of the musculoskeletal structure." The results of modeling the response of one subject suggest that certain anatomical structures (such as the arms and shoulders) become more reactive in the first resonance region at the higher acceleration level. It is not known whether this assumption can be applied to the responses of the remaining subjects. The redistribution of the upper torso/spine masses could be a consequence of describing a relatively complex biological structure as a lumped-mass system. For example, the spinal column was modeled as a single lumped subsystem in the preliminary model. Researchers, including Panjabi et al. (1986) and Hagena et al. (1986), have observed transmissibility peaks in the lumbar spine between 4 and 8 Hz. Hagena et al. (1986), although observing relatively high transmissibility peaks in the thoracic spine at about 18 Hz, concluded that the independent resonance of the spine occurred between 7 and 10 Hz. These findings do suggest that the spine should be modeled with additional coupled subsystems but that additional data on spinal column motion are needed.

The elimination of the second magnitude peak between 7 and 9 Hz in the majority of the impedance profiles collected at 0.694 and 1.734 ms^{-2} rms implied that there was increased damping in the legs at these higher acceleration levels. The modeling results also showed that the undamped natural frequency of the legs decreased with increasing acceleration and fell within the frequency range of region one as depicted in Table 1, particularly at the highest acceleration level. Again, Fairley and Griffin (1989) did show that the legs could affect the magnitude of the first resonance peak in the apparent mass response. From the results of this study, it was difficult to determine to what extent the changes in the stiffness and damping characteristics of the legs affected the observed response in the first region. The preliminary modeling effort assumed that the motions of subsystem three, the major contributor to the first region of resonance, was coupled to the motions of the spine. The mass, stiffness, and damping characteristics of both subsystems two and three changed with the acceleration level, which would influence the characteristics of the first peak. Using the base-excited, 5DOF model, it can be shown, however, that lowering the undamped natural frequency of the legs to coincide more closely with that of the chest/shoulders subsystem will increase the magnitude of the first peak. Increasing the damping of the legs will affect the extent of this increase. In addition, changing the stiffness and damping characteristics of the legs will also influence the magnitude of the remaining resonance peaks, which further complicates the evaluation of resonance behavior using the impedance technique.

The data collected in this study further supports the occurrence of nonlinear behavior in the response of the human to whole-body vibration and suggests that, for relatively large differences in the acceleration level, changes in the mass, stiffness, and damping characteristics of the human body may be statistically significant. The preliminary assessment of the nonlinear impedance response of the human also suggests that the load transmission/attenuation characteristics associated with changes in the loading environment may be quantitated with the use of an appropriate model. To determine the significance of these changes, the model should be applied to generate the mass, stiffness, and damping characteristics for all 48 impedance profiles collected in this study, and the results statistically compared between subjects and between acceleration levels. This will require an improved

scheme, similar to that used by Smith and Kazarian (1994) for identifying the unknown model parameters. In addition, although the results of others do support some of the assumptions made for the preliminary modeling of impedance, further information is needed to validate these assumptions or provide information that would improve the model, particularly in trying to derive an anatomically correct dynamic model. Transmissibility data has recently been collected in this laboratory and should provide valuable information about the biodynamic behavior of the legs and the spine, particularly under the testing conditions used in this laboratory. The model should ultimately be capable of simulating both the impedance and transmissibility responses of the whole body and the major anatomical structures contributing to the measured results. Establishing the mass, stiffness, and damping characteristics of specific anatomical regions or structures sensitive to the vibration loading environment will contribute to optimizing design criteria for vibration isolation systems including vehicle suspensions and seats.

The author acknowledges the assistance of the University of Dayton Research Institute, particularly Mr. Fred Davis, for facility operation support. The author would also like to extend her appreciation to Dr. Vernon H. Neubert, Professor Emeritus, The Pennsylvania State University, Department of Engineering Science and Mechanics; and to Dr. Ints Kaleps, Chief, Vulnerability Assessment Branch, Armstrong Laboratory, Wright-Patterson AFB, OH for their valuable comments and suggestions.

REFERENCES

Broderson, A. B., and von Gierke, H. E., 1971, "Mechanical Impedance and Its Variation in the Restrained Primate During Prolonged Vibration," *ASME 71-Wa/BHF-8,* pp. 1–9.

Coermann, R. R., Ziegenruecker, G. H., Wittwer, A. L., and von Gierke, H. E., 1960, "The Passive Dynamic Mechanical Properties of the Human Thorax–Abdomen System and of the Whole Body System," *Aerospace Medicine,* Vol. 31, pp. 443–455.

Coermann, R. R., 1961, "The Mechanical Impedance of the Human Body in Sitting and Standing Position at Low Frequencies," *ASD Technical Report 61-492,* Wright Patterson AFB, OH, pp. 1–40.

Fairley, T. E., and Griffin, M. J., 1989, "The Apparent Mass of the Seated Human Body: Vertical Vibration," *Journal of Biomechanics,* Vol. 22, pp. 81–94.

Guignard, J. C., 1972, "Biodynamics," in J. C. Guignard, and P. F. King, *Aeromedical Aspects of Vibration and Noise (AGARD-AG-151),* Technical Editing and Reproduction Ltd, Harford House, London, Chap. 4, pp. 29–35.

Guignard, J. C., and Irving, A., 1960, "Effects of Low Frequency Vibration on Man," *Engineering,* Vol. 190, pp. 364–367.

Hagena, F. W., Werth, C. J., Piehler, J., Plitz, W., Hofmann, G. O., and Zwingers, Th., 1986, "In-Vivo Experiments on the Response of the Human Spine to Sinusoidal G_z—Vibration," *Backache and Back Discomfort, AGARD Conference Proceedings (AGARD-CP-378),* pp. 16-1–16-12.

Hinz, B., and Seidel, H., 1987, "The Nonlinearity of the Human Body's Dynamic Response During Whole Body Vibration," *Industrial Health,* Vol. 25, pp. 169–181.

International Organization for Standardization, 1985, "Guide for the Evaluation of Human Exposure to Whole-Body Vibration—Part I: General Requirements," *ISO 2631-1985.*

International Organization for Standardization, 1981, "Vibration and Shock—Mechanical Driving-Point Impedance of the Human Body," *ISO 5982-1981.*

International Organization for Standardization, 1987, "Vibration and Shock—Mechanical Transmissibility of the Human Body in the Z-Direction," *ISO 7962-1987.*

Mertens, H., 1978, "Nonlinear Behavior of Sitting Humans Under Increasing Gravity," *Aviation, Space and Environmental Medicine,* Vol. 49, pp. 287–298.

Neubert, V. H., 1987, *Mechanical Impedance: Modelling/Analysis of Structures,* Jostens Printing and Publishing Company, State College, PA.

Panjabi, M. M., Andersson, G. B., Jorneus, L., Hult, E., and Mattsson, L., 1986, "In Vivo Measurements of Spinal Column Vibrations," *Journal of Bone and Joint Surgery,* Vol. 68-A, pp. 695-702.

Slonim, A. R., 1981, "Some Vibration Data on Primates Implanted with Accelerometers on The Upper and Lower Spine: Methodology and Results in Rhesus Monkeys," *AFAMRL-TR-81-153,* pp. 1–81.

Smith, S. D., 1992, "Impedance Response Characteristics of the Primate *Mucaca mulatta* Exposed to Seated Whole-Body g_z Vibration," *Journal of Biomechanics,* Vol. 25, pp. 839–847.

Smith, S. D., and Kazarian, L. E., 1994, "The Effects of Acceleration on the Mechanical Impedance Response of a Primate Model Exposed to Sinusoidal Vibration," *Annals of Biomedical Engineering,* Vol. 22, No. 1, pp. 78–87.

U.S. Department of Defense, 1981, "Human Engineering Design Criteria for Military Systems, Equipment and Facilities," *Military Standard 1472C,* Government Printing Office, Washington, D.C.

Wilder, D. G., Woodworth, B. B., Frymoyer, J. W., and Pope, M. H., 1982, "Vibration and the Human Spine," *Spine,* Vol. 7, pp. 243–254.